A Weather-Type Approach to Analyzing Winter Precipitation in France: Twentieth-Century Trends and the Role of Anthropogenic Forcing

J. BOÉ AND L. TERRAY

Climate Modelling and Global Change Team, CERFACS/CNRS, Toulouse, France

(Manuscript received 1 December 2006, in final form 19 November 2007)

ABSTRACT

The relationship between large-scale atmospheric circulation and November–March precipitation over France during the twentieth century is investigated. A long daily MSLP dataset is used to derive daily weather types that are discriminant for precipitation. A linear regression model is then used to relate the November–March-accumulated precipitation amount and the occurrence frequency of the weather types. This simple model shows that an important part of the interannual variability of precipitation is directly linked to large-scale circulation changes. Trends in observed precipitation and precipitation series reconstructed by regression are computed and compared. Spatially coherent trends in November–March precipitation during the second half of the twentieth century are observed, with an increase in the north and a decrease in the south. The spatial pattern of the trends in reconstructed precipitation is very similar to that observed, even if an underestimation of the positive trends in the north is seen, indicating that other mechanisms play a role. A detection study then leads to a better understanding of the respective roles of anthropogenic forcing (greenhouse gases and sulfate aerosol) and sea surface temperature in the evolution of the weather-type occurrence. Finally, it is shown that intratype dynamical variability has also played a role in precipitation changes in northern France, whereas no impact of temperature changes is seen.

1. Introduction

Large uncertainties in changes in precipitation under anthropogenic climate change still exist, especially at the regional scale. A better understanding of the physical mechanisms underlying the spatiotemporal variability of precipitation at the regional scale in the present climate is needed to progress. In France, spatially coherent trends in winter precipitation during the second half of the twentieth century have been observed (Moisselin et al. 2002). The pattern is characterized by an increase of precipitation in the north and a decrease in the south of the country. In the global change context, understanding the causes of these trends, and whether they may be related to anthropogenic forcing, is of particular interest.

The relationship between large-scale circulation (LSC) and precipitation over western Europe has been emphasized for a long time. The North Atlantic Oscillation (NAO) is well known to influence precipitation over Europe, especially in the northwestern part of the continent (Hurrell 1995). More specifically, several studies have highlighted the links that exist between atmospheric circulation patterns and precipitation for different western European countries [e.g., see Trigo and DaCamara (2000) for Portugal, Goodess and Jones (2002) for the Iberian Peninsula, Plaut et al. (2001) and Sanchez-Gomez and Terray (2005) for France, Fowler and Kilsby (2002) for the United Kingdom, and Xoplaki et al. (2004) for the Mediterranean basin]. Possible modifications to the atmospheric circulation resulting from climate change may thus have impacts on European precipitation. For example, given the conclusions of Terray et al. (2004), who showed that the end-of-century anthropogenic climate change over the North Atlantic–European region strongly projects onto the positive phase of the NAO during wintertime, dynamical changes in precipitation over Europe may be expected. Regarding the late twentieth century, Goodess and Jones (2002) have shown that an important part of the changes in winter precipitation for the Iberian Peninsula can be explained by the modification of the occurrence frequency of a few weather types (WTs).

Corresponding author address: J. Boé, Climate Modelling and Global Change Team, CERFACS/CNRS, 42 Avenue Gaspard Coriolis, Toulouse 31057, France.
E-mail: boe@cerfacs.fr

DOI: 10.1175/2007JCLI1796.1

Others studies have come to a similar conclusion [see, e.g., Paredes et al. (2006), regarding March precipitation in Spain and Portugal].

The causes of the changes in LSC over Europe remain unclear. It is not known whether these changes simply are due to natural climate variability (Stephenson et al. 2000) or whether they are a signature of anthropogenic climate change (Corti et al. 1999). Applying a detection and attribution framework is probably the best way to answer this question. During the last decades, important progress has been made on climate change detection and attribution (Barnett et al. 2005). In particular, the role of anthropogenic greenhouse gases (GHGs) in the evolution of global temperature (Stott et al. 2001) is now well established. Other studies regarding global precipitation (Lambert et al. 2004) or mean sea level pressure (MSLP) in the North Atlantic sector (Gillett et al. 2003, 2005) have also concluded that anthropogenic forcing impacts the evolution of these variables. A detection framework can also test whether a model has a realistic response to anthropogenic forcing for a particular variable, which is an important question in the context of climate change impact studies. Whereas the skills of regional climate models (RCMs) or a variable-resolution atmospheric model are now sufficient to proceed to detection and attribution studies on temperature at the regional and even subregional scale (Spagnoli et al. 2002), the generally poor simulation of precipitation by these models may still be problematic for the detection of the influence of anthropogenic forcing on regional precipitation.

The first objective of this work is to explore to what extent the atmospheric circulation explains the interannual variability and the trends in November–March precipitation in France. The atmospheric circulation will be described in terms of the occurrence frequency of a few WTs. The second objective is to test if the changes in WT occurrence frequency may be linked to anthropogenic forcing. After introducing the data and the model used in the study (section 2) and briefly describing the main characteristics of winter precipitation in France (section 3), we introduce a daily weather-typing scheme, which is discriminant for precipitation in France (section 4). The relationships between the WTs and precipitation at the interannual level are investigated in section 5. The trends in precipitation and WT occurrence frequencies are studied in section 6. Section 7 is dedicated to a detection study of the impact of anthropogenic forcing on changes in precipitation and WT occurrence frequency. Section 8 is dedicated to the question of the role of intratype and thermodynamical changes on precipitation evolution. The main conclusions of the study are presented in section 9.

2. Data and model

Weather typing is an efficient approach to study the relationship between LSC and regional climate; it requires a LSC variable at the daily time step. Moreover, a long dataset is necessary to draw robust conclusions. The newly available daily gridded mean sea level pressure (MSLP) dataset from the European Community–funded European and North Atlantic Daily to Multidecadal Climate variability (EMULATE) project is a great opportunity for this type of study. This dataset (EMSLP) covers the North Atlantic–European sector (25°–70°N, 70°W–50°E) with a 5° latitude × 5° longitude grid and extends back to 1850 (Ansell et al. 2006).

Daily precipitation observations come from the Série Quotidienne de Référence (SQR) Météo-France dataset and the monthly series of precipitation and temperatures are from the Série Mensuelle de Référence (SMR) Météo-France dataset (Moisselin et al. 2002). In the two dataset the same stations are available (308 series for precipitation and 91 for temperature) from as early as 1873 for some stations. A specific dataset is used at the monthly level because the monthly series have been homogenized (Mestre 2000). This procedure was intended to detect and correct homogeneity breaks and outliers resulting from, among other causes, changes in the location of station observations or changes of instrumentation. The monthly series thus constitute a high-quality dataset that is well adapted to studies of temporal variability and trends. Nevertheless, because of the homogenization procedure requirements and the availability and quality of observations, a homogeneous spatial coverage of the French territory cannot be performed for precipitation and this is a limitation of our study. A subset of 299 precipitation stations with no missing values for the 1900–2000 period is extracted. The domain chosen for MSLP (hereafter D1) and the localization of the French precipitation stations with the orography are shown in Fig. 1. For precipitation over Europe, the Climatic Research Unit (CRU) time series (TS) 2 monthly dataset is used (Mitchell et al. 2004).

The global atmospheric general circulation model (AGCM) used in this study is the variable-resolution new version of the Météo-France Action de Recherche Petite Echelle Grande Echelle (ARPEGE) atmospheric model (Gibelin and Déqué 2003). The model uses semi-Lagrangian advection and a two time-level discretization. Vertical discretization uses hybrid coordinates with 31 vertical levels. It has a T106 spectral

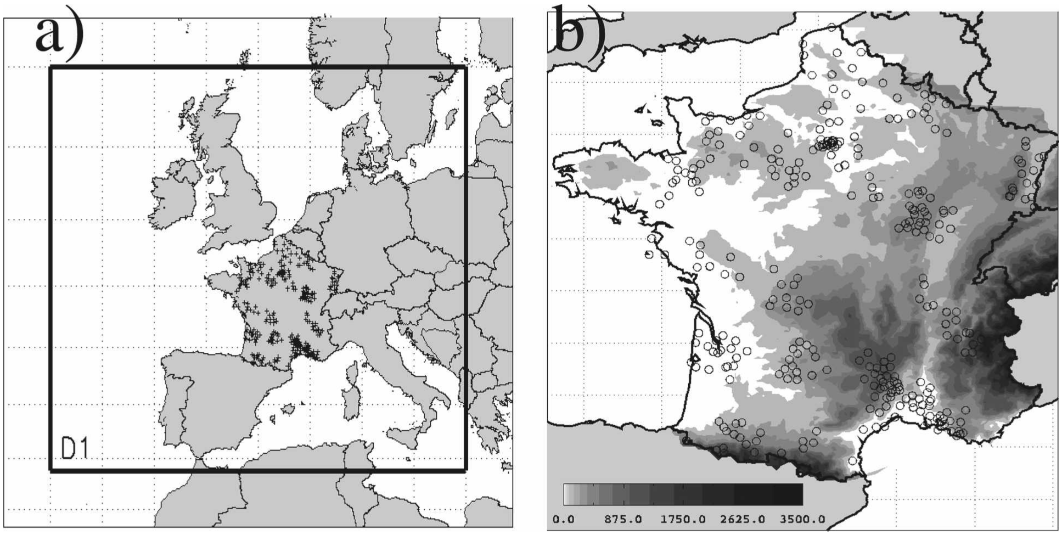

FIG. 1. Domain for (a) MSLP (D1) and (b) precipitation stations with French relief (altitude: m).

truncation. The variable resolution allows one to increase both the spectral and gridpoint resolution over a given region of interest. In the present case, the center of the high-resolution region is located in the middle of the Mediterranean basin. The highest horizontal resolution is about 0.5° and remains fairly high over the entire North Atlantic–European sector.

Four ensembles of six forced atmospheric simulations for the 1950–2000 period with different sets of forcing are used. In the first one (S), the AGCM is forced by the observed sea surface temperature (SST; Smith and Reynolds 2004) alone [GHG and sulfate aerosol (SUL) concentrations are kept constant at the 1950 level]. In the second one (SG), the model is forced by observed SST and GHG concentrations. In the third one (SGS), the model is forced by observed SST, GHG, and SUL concentrations. In the last one (SGSN), natural forcing (solar and volcanic) is added to all of the previous forcings.

As mentioned in the introduction, a main objective of this paper is to understand the causes of the large trends that are seen in winter precipitation over some areas of France. In the following sections, the analysis is focused on an extended winter season, from November to March. We use these two additional months in the analysis because the trends, circulation patterns, and links between the circulation patterns and the regional climate during these months are coherent with those obtained during the traditional winter.

3. Precipitation characteristics

To begin, November–March precipitation properties in France are examined. Figures 2a,b depict the mean and the standard deviation of November–March-accumulated precipitation amounts, respectively. An important spatial variability exists, which is partially linked to the orography (already shown in Fig. 1b). The amount of precipitation and its variability are smallest in the northwestern region. Some areas in the south and some stations in the northeast exhibit large seasonally cumulated amounts associated with a strong variability.

Figure 2c displays the trend in November–March precipitation in the 1951–2000 period relative to the 1900–2000 average. The associated p values of the significance test [i.e., the test of the slope parameter; see von Storch and Zwiers (1999)] are shown in Fig. 2d. A north–south contrast in the trends is observed, with significant positive trends in northern France and negative trends in the south. For many stations of the indented region in the southeastern part of the country [the Languedoc-Roussillon and Bouche du Rhone (LRB) region], very pronounced negative trends are seen, with decreases greater than 35% of the 1900–2000 mean for some stations. The null hypothesis of a zero trend cannot be rejected for all of these stations, partly because of the strong interannual variability of precipitation in this area. It is nevertheless worthwhile to try to understand the possible drivers of the trends in the LRB region because they are very pronounced and may have important impacts on water resources. These results can be considered in a more general context: Zhang et al. (1997) noted a general decline in winter precipitation in the northern Mediterranean Basin. Norrant and Douguédroit (2006) also noted decreasing trends in the 1950–2000 period over the Mediterranean area, especially during winter, although they are rarely signifi-

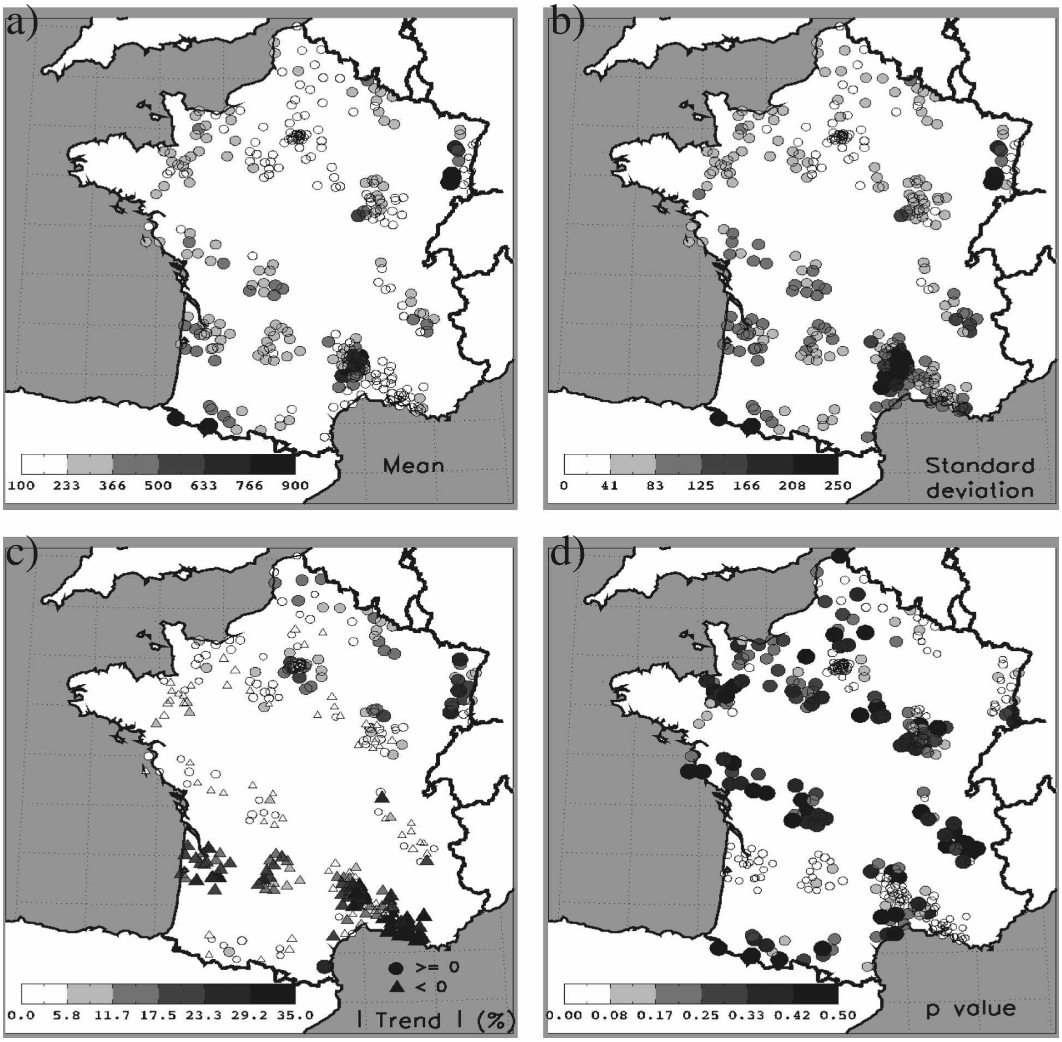

FIG. 2. November–March-accumulated precipitation amounts in the 1900–2000 period: (a) mean and (b) std dev; (c) 1951–2000 trend in the November–March-accumulated precipitation amounts as a percent of the 1900–2000 mean; and (d) p value of the significance test on the trends (see text).

cant. Corte-Real et al. (1998) and Trigo and DaCamara (2000) characterized a strong decline of precipitation in March over the Iberian Peninsula.

We are first interested in understanding to what extent the trends and, in particular, the north–south contrast can be explained by changes in the LSC.

4. Derivation of the WTs

To study the relationship between LSC and precipitation over France, a weather-typing approach is followed for the November–March period. The WTs are derived using clustering analysis through the k-means automatic partitioning algorithm (Michelangeli et al. 1995). Plaut et al. (2001) showed that accounting for precipitation properties during the classification process gives WTs that are more discriminant for precipitation. In our case, a two-variable-state vector is used for the classification. The first 10 principal components (PCs) of MSLP and the first 10 PCs of the square root of French precipitation are concatenated, giving a state vector in a 20-dimensional space. The spatial domain used for MSLP (D1) and the localization of the precipitation stations have already been shown in Fig. 1. A weighting of the state vector is applied in order to give the same weight to the first PC of MSLP and the first PC of precipitation. The difference of weight between the first PC and the nine other PCs of each field is maintained, given their respective standard deviations. The k-means algorithm gives the centroids of the clusters in the 20-dimensional space, accounting for both MSLP and precipitation. Because the objective is to obtain a final classification that only depends on the LSC, only the 10 coordinates of the centroids that correspond to MSLP are finally used to define the WTs. Each day is then reclassified to the nearest WT, in terms of Euclidean distance on MSLP. The major drawback of the k-means algorithm is that the number k of clusters must be chosen a priori. Different approaches are used to determine the optimal number k of clusters, but no consensus exists. Here, a test based on an inter/intracluster variance ratio described in Straus and Molteni (2004) has been used, giving an optimal partition with eight clusters. The stability of the partition has been checked by repeating the cluster analysis with different initial seeds. The overall similarity of the different partitions obtained gives confidence in the robustness of the clusters. Figure 3 shows the composite MSLP anomalies of the days belonging to each WT and the ratio between mean precipitation for the days within the clusters and the global seasonal mean.

Figure 3 demonstrates that the WTs, although based on a low-resolution MSLP dataset, are efficient in discriminating localized precipitation patterns in France. WT2, the most frequent WT, a blocking-like pattern, is characterized by very dry conditions over the whole domain. WT3, WT4, WT5, although quite similar in terms of MSLP patterns, with pronounced negative MSLP anomalies in the north of D1, nevertheless have different regional effects on precipitation. WT3 produces intense rainfall (3 times more than the seasonal mean) over the entire territory, except for some stations in the LRB region; whereas WT4 gives very intense precipitation in the LRB region but less intense precipitation in the extreme north and the Pyrenees (mountainous area located in southwestern France). WT5 is dry in all of the LRB area and is very wet in the north.

Precipitation in the LRB region exhibits a particular behavior, which is often different from the rest of the country. This characteristic is particularly evident for WT6, which is dry everywhere except in the LRB region. Moreover, very small-scale spatial variability exists in this area (visible, e.g., for WT3 and WT5). This region is both influenced by flows from the Atlantic Ocean and the Mediterranean Sea and has a complex topography (see Fig. 1). It is more or less protected from westerly and northwesterly flow (as for WT3 and WT5) by the Massif central, the mountainous area in the center of France, whereas southerly flows can produce intense rainfall (WT4 and WT6).

Although the WTs have been constructed to be especially discriminant for precipitation over France, they show similarities with circulation types used in other studies, as Trigo and DaCamara (2000) and Goodess and Jones (2002). For example, WT6 and WT4 are similar to the central and southwest circulation types of these studies, respectively. Interestingly, Trigo and DaCamara (2000) linked the decreasing trend of rainfall over Portugal in March over the period of 1946–90 to the decreasing frequency of the central and southwest circulation types (among others). Our results are also coherent with previous studies dedicated to rainfall over regions of France, such as Plaut et al. (2001) and Sanchez-Gomez and Terray (2005).

5. Regression analysis

The relationships between WT occurrence frequency and the November–March precipitation are now studied at the interannual level. High linear correlations between the mean of November–March WT occurrence frequency and cumulative precipitation are obtained for some WTs (see Fig. 4; there are correlations of about -0.6 for WT2 everywhere, and of about -0.6 for WT5 in the north, for WT6 in the LRB region, and for WT3 over the entire domain except the LRB region).

To explore to what extent the spatiotemporal variability of November–March precipitation can be explained by changes in WT occurrence frequency, a least squares multiple linear regression analysis is performed for each precipitation station. The November–March occurrence frequencies of the WTs, except WT8, are used as predictors, whereas the predictand is the accumulated precipitation amount. WT8 is not used as predictor in the regression equation in order to avoid the problem of multicolinearity (von Storch and Zwiers 1999). Because the link between precipitation and WT8 is weak, this choice does not result in a significant loss of information. Precipitation and WT occurrence frequency series are first filtered to remove subdecadal fluctuations in order to avoid obtaining spurious results due to similar low-frequency trends. A running average with a 13-weights window [1/576(1–6–19–42–71–96–106–96–71–42–19–6–1)] is used. The low-pass-filtered series are then removed from the original series and the regression equation is solved for the residual series. To ensure the robustness of our model coefficients, we have applied a cross-validation procedure. The correlation coefficient between the original and reconstructed series is displayed for three time periods for each station (Fig. 5). A high correlation coefficient (around 0.80) is obtained over most of France, except for some stations in the south, where it is between 0.4 and 0.6. In the LRB region and in the extreme north of

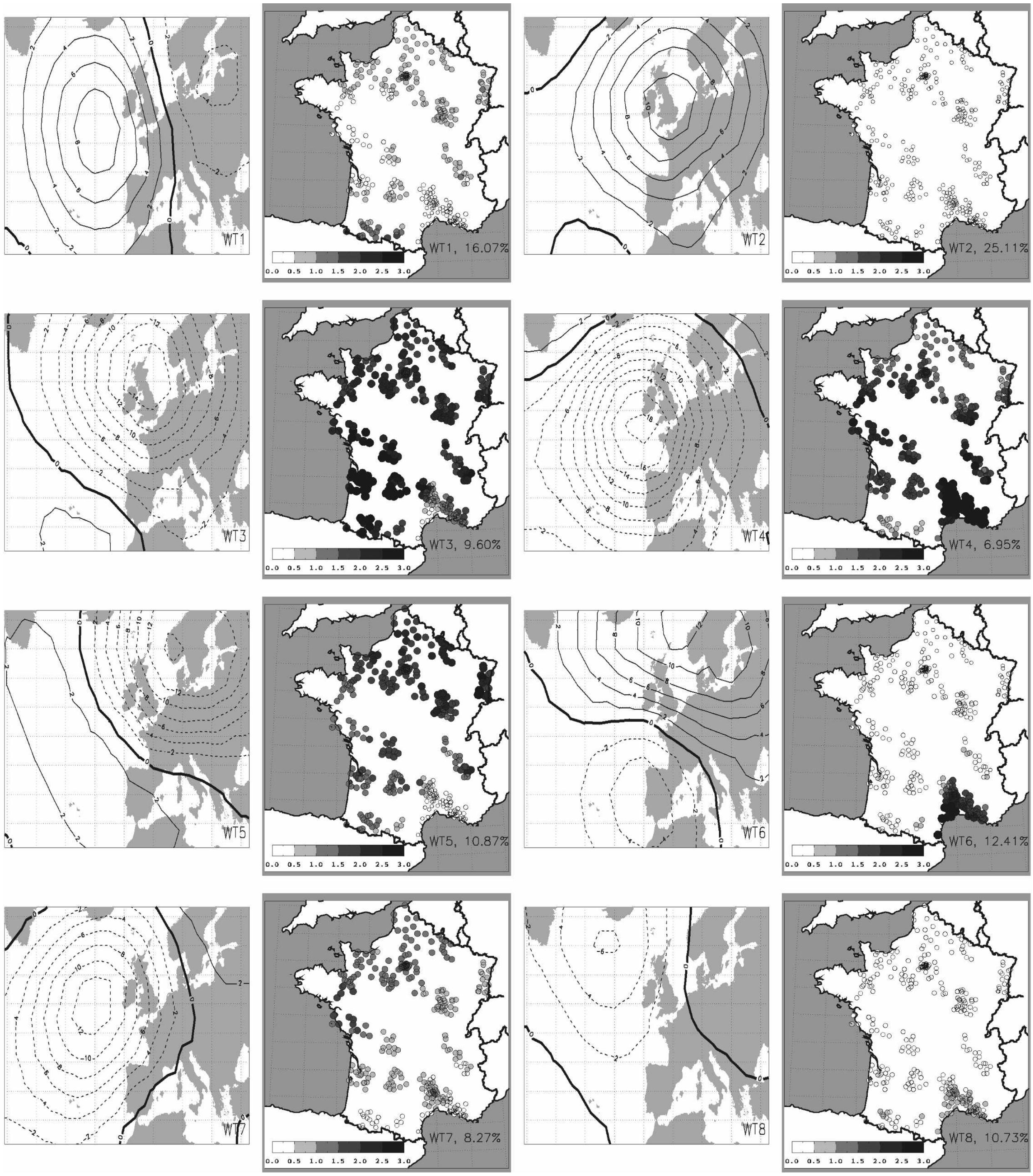

FIG. 3. WTs and associated precipitation: (left) MLSP composite anomaly of the days belonging to each WT (hPa) and (right) ratio of precipitation composite and seasonal average precipitation (no dimension). WT occurrence frequency is indicated on the precipitation map.

the country greater correlations exist in the 1951–2000 period. The discrepancy between the two subperiods may be explained by problems with regard to MSLP or precipitation series at the beginning of the period, or nonstationarity of the relationship between precipitation and the WTs. Note that the results are insensitive to the preprocessing filtering step. By either not filtering or removing a simple linear, quadratic, or cubic trend before the regression analysis, results that are quasi identical to those shown in Fig. 5 are given.

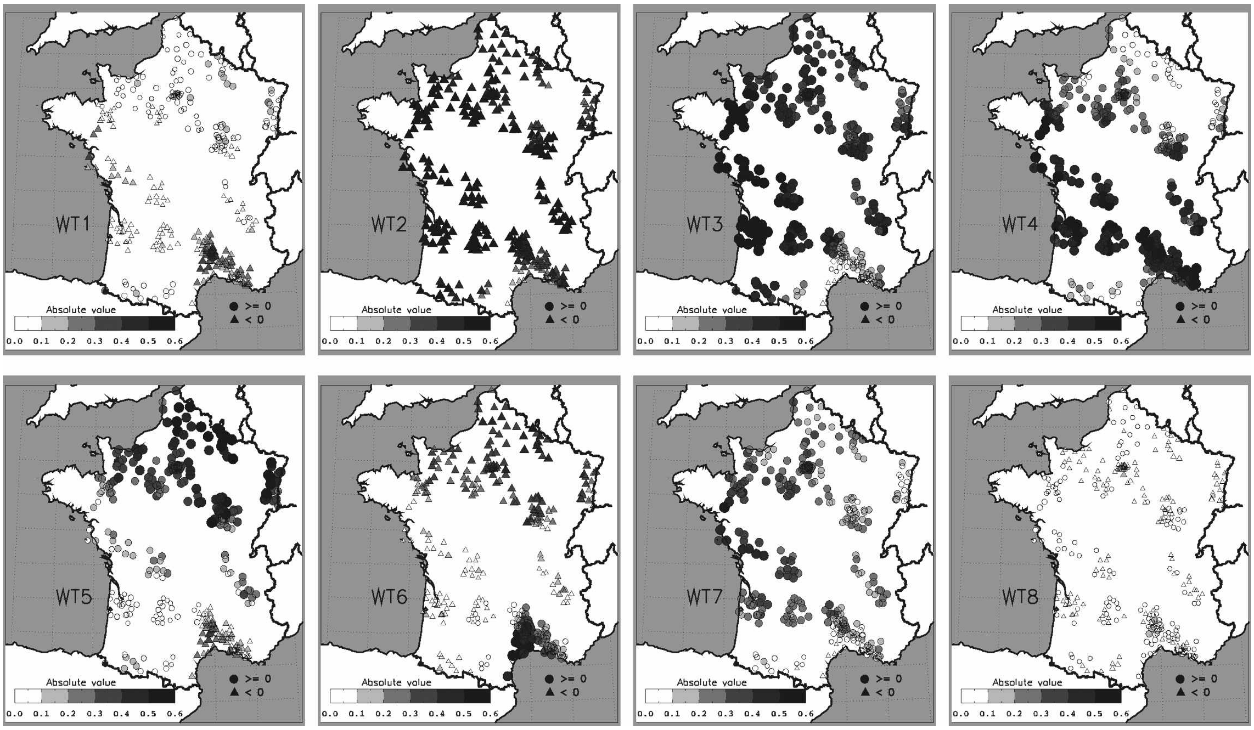

FIG. 4. Linear correlation between November–March mean WT occurrence frequency and November–March-accumulated precipitation amount. The color scale shows the absolute value of the correlation. The symbols give the sign of the correlation (circle for positive correlation and triangle for negative correlation).

Therefore, for the following analyses, filtering is not applied.

The WTs have been constructed to be especially discriminant for November–March precipitation over France. Nevertheless, given their spatial patterns, they could also be relevant for all of western Europe. To test this, similarly to Fig. 5, Fig. 6 displays the results of the cross-validation regression analysis over Europe using the CRU TS 2 dataset for precipitation. Figure 6 demonstrates that the WTs are also discriminant for precipitation over a large part of western Europe (Spain, the United Kingdom, and Norway), whereas the skill of

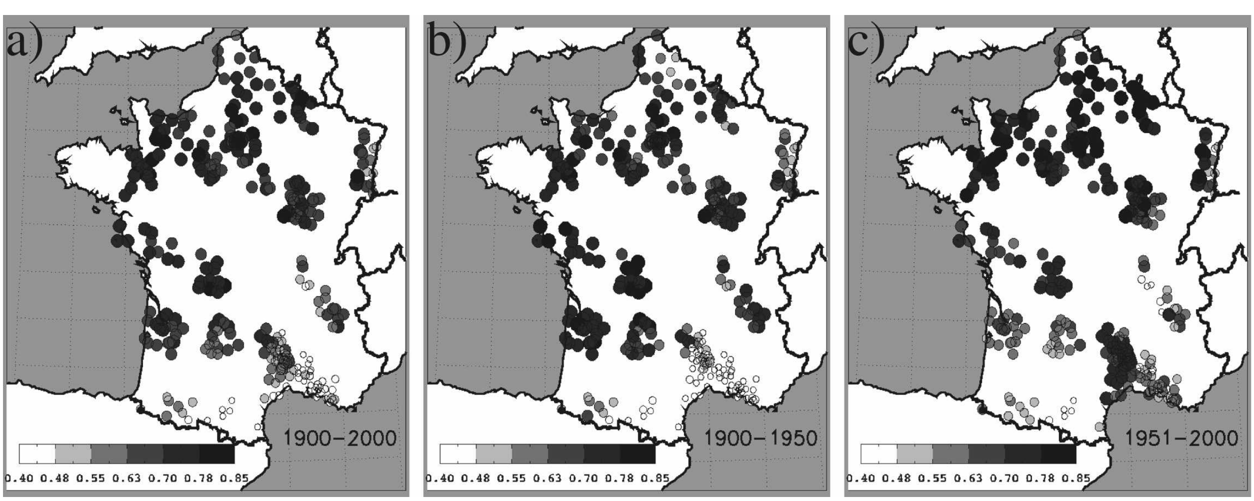

FIG. 5. Linear correlations between reconstructed and observed precipitation for each station for three time periods: (a) 1900–2000, (b) 1900–50, and (c) 1951–2000.

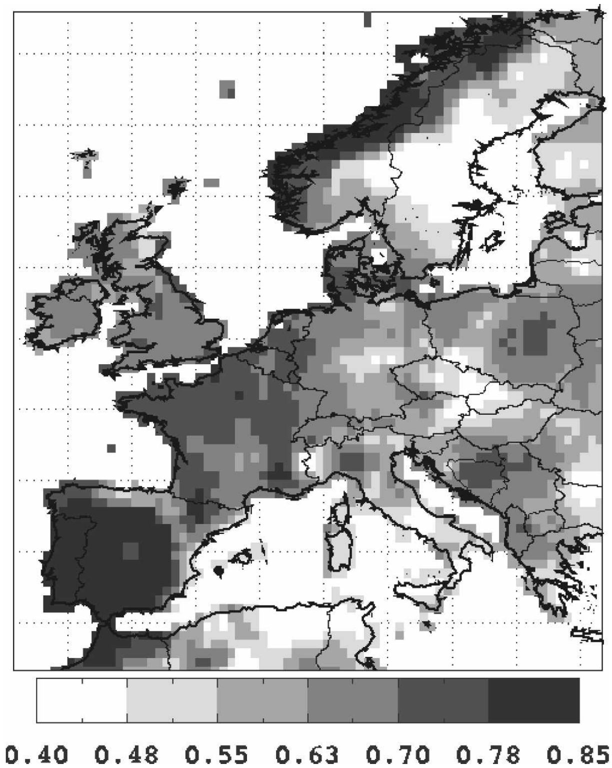

FIG. 6. Linear correlations over the 1951–2000 period between reconstructed and observed precipitation over Europe (CRU TS 2 dataset).

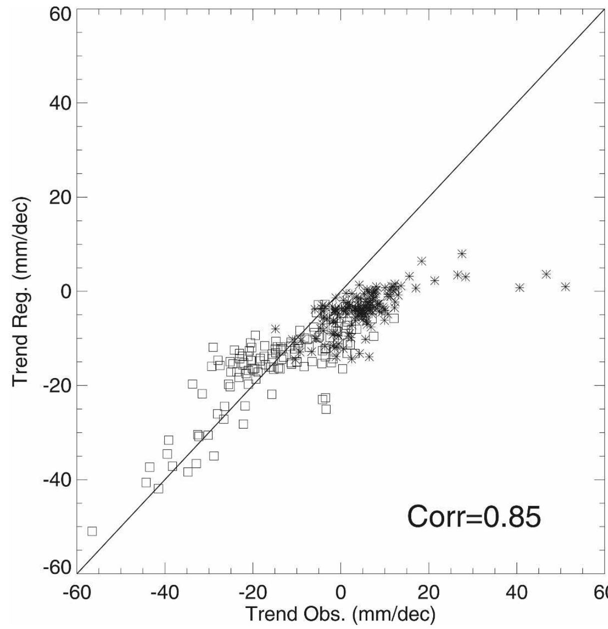

FIG. 7. Observed vs reconstructed trends (mm decade^{-1}) in precipitation for the 1951–2000 period. The black line corresponds to the $y = x$ equation; the squares (stars) are the stations in the south (north) with a latitude lower (greater) than 46°N.

the regression model is more limited in the eastern part of the domain. Some of the conclusions of this study may therefore also be relevant for western Europe.

6. Trend analysis

Linear trends for the 1951–2000 period are computed on the series obtained by the regression analysis with WT occurrence frequencies as predictors, and are compared to the observed trends already shown in section 2 (Fig. 7).

For the stations with strong negative trends (all located in the south; see Fig. 3), a very good match is seen between the reconstructed and observed values. For the stations with significant positive trends (located mainly in the northeast), the reconstructed trends are underestimated. The correlation between the map of observed and reconstructed trends is 0.85, indicating that the use of WTs gives a good representation of the spatial pattern of precipitation trends in France.

We also test whether the low-frequency component in the precipitation series is correctly reproduced by the regression model. The low-pass filter already described in the previous section is used to extract the low-frequency component (corresponding roughly to decadal and greater variations) from the observed and reconstructed series. The two series are then correlated for each station. Results for the entire period and two subperiods are displayed in Fig. 8.

The simple linear regression model well captures the observed low-frequency variations of precipitation. However, in the 1951–2000 subperiod (Fig. 8c), for some stations located in northeastern France, a decrease of the correlations is seen. This is consistent with what has been previously found regarding the underestimation of trends in northeastern France in this period. To understand the changes in precipitation, the trends in WT occurrence frequency are computed for the 1951–2000 period (Fig. 9). Some WTs exhibit large trends. The occurrence frequency of WTs that are positively correlated to precipitation in the LRB region all decrease (WT6, WT4, and WT3), whereas the WTs that become more frequent are dry in the LRB region (WT1 and WT5) but wet in the north (WT5, and WT1 to a lesser extent) or dry everywhere (WT2). For WT2, WT3, WT4, and WT5 the trends are significant at the 0.1 level (0.05 for WT3, WT4, and WT5). The changes in WT occurrence frequency thus provide a good physical explanation for the trend pattern in precipitation, in particular the north–south contrast.

In accordance with previous studies in other western European countries (Goodess and Jones 2002; Trigo

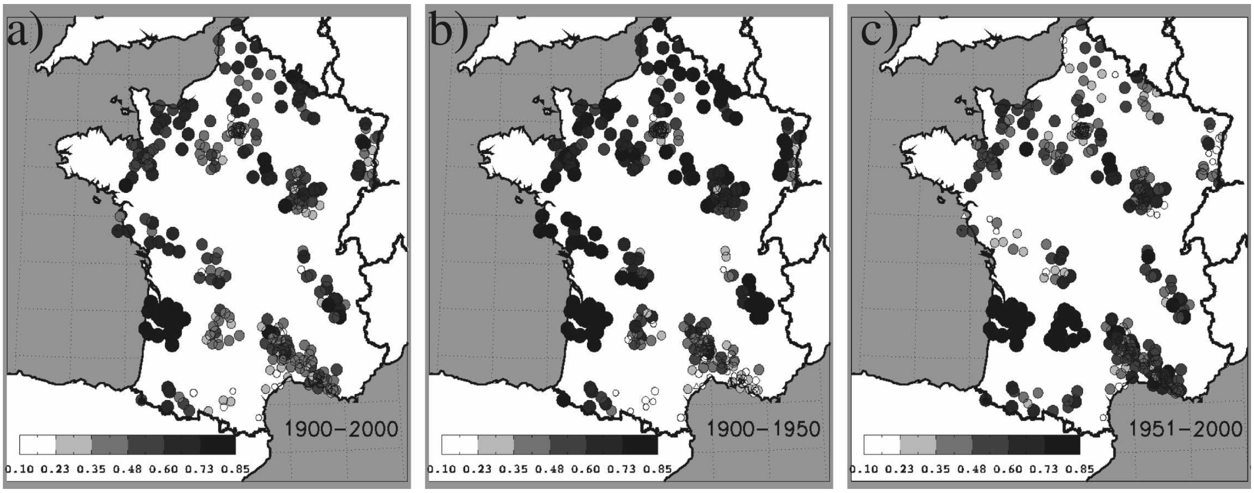

FIG. 8. Linear correlations between low-pass-filtered reconstructed and observed precipitation for each station for three periods: (a) 1900–2000, (b) 1900–50, and (c) 1951–2000.

and DaCamara 2000), we have shown that an important part of the interannual variability in winter precipitation in France can be explained by the variability in the occurrence frequency of a few WTs. Moreover, an important part of the trends in precipitation in the second half of the twentieth century can also be explained by only considering the changes in WT occurrence frequency. However, because the changes in the WT occurrence frequency do not explain the full variability and trends in precipitation, it is important to find which other(s) mechanism(s) play a role. Additionally, can the modifications in WT occurrence frequency and the changes in precipitation be explained by intrinsic atmospheric variability alone, or does anthropogenic forcing play a role? This question is the object of the next section.

7. Detection of external influence on precipitation and WT occurrence frequencies

a. Methodology

In this section we use an optimal detection methodology (Allen and Tett 1999) to test whether anthropogenic forcing has played a role in the trends in precipitation over France and in the changes in WT occurrence frequency. The global variable-resolution

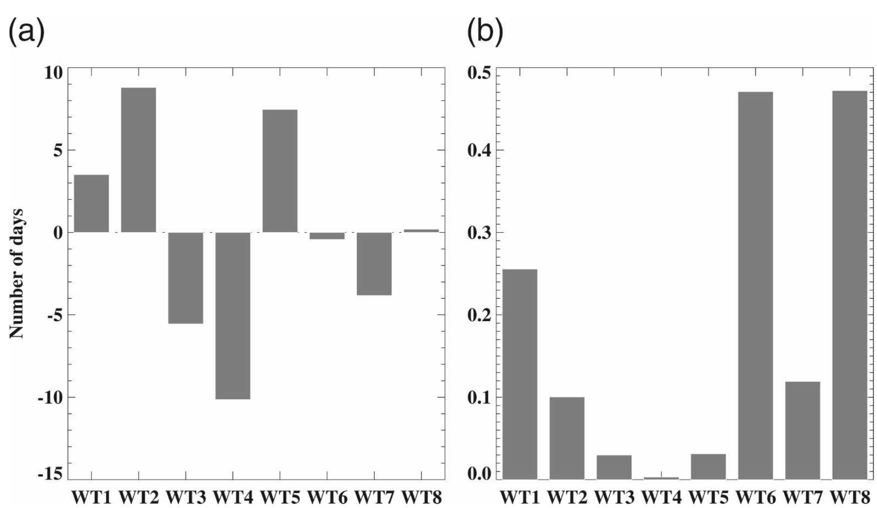

FIG. 9. (a) The 1951–2000 trends in November–March WT occurrence frequencies (difference from the 1900–2000 average in number of days) and (b) the p values of the significance test of the slope parameter are shown.

AGCM used in this study has a high resolution of about 60 km over France, and thus is suitable to study precipitation at regional and subregional scales. Moreover, as argued by Sexton et al. (2001), the noise is less in a forced AGCM approach than in a coupled ocean–atmosphere general circulation model approach, because the variations resulting from changing SSTs no longer contribute to climate noise. Detection may thus be facilitated for some variables. The main limitation of the forced framework is that the possible effects of changes in SST resulting from anthropogenic forcing on the atmosphere are not detectable as being anthropogenic. The optimal detection algorithm used in this study is described in Allen and Tett (1999) and Tett et al. (2002) and is briefly summarized in the appendix. We focus on anthropogenic forcing only and do not try to separate GHG and SUL influences. Intraensemble variability from the four ensembles of six simulations described in section 2 is used to estimate the internal (or natural) variability. In the following analysis, the considered period is 1950–2000.

b. Results

The first time, the optimal detection algorithm is used to try to directly detect an anthropogenic influence on precipitation over France. The detection vector is first formed using the decadal means of November–March precipitation in France. The residuals of the regression do not satisfy the consistency test proposed by Allen and Tett (1999) at all truncations, suggesting a bias in model variability. Similar results are obtained for 50- and 30-yr trends as detection vectors. Thus, no conclusions can be drawn from the direct detection study on precipitation; either precipitation might be too poorly simulated by the model or other influences that are not taken into account in our study might play a role.

The second time, the optimal detection algorithm is used to try to detect an external influence on the WT occurrence frequency. First, the ability of the ARPEGE AGCM to correctly represent the mean occurrence frequency is tested. MSLP from the ARPEGE model is first projected on the EOF derived from the EMSLP dataset. The resulting series are then used to classify each day of the model run as one of the eight WTs. As shown by Fig. 10, the model well reproduces the mean WT occurrence frequencies. The spatial patterns of the WTs in ARPEGE are similar to those found in EMSLP (not shown; spatial correlation always greater than 0.90).

The five decadal means of the WT occurrence frequency in the 1950–2000 period are used as a detection vector. Under the hypothesis that the combined signal

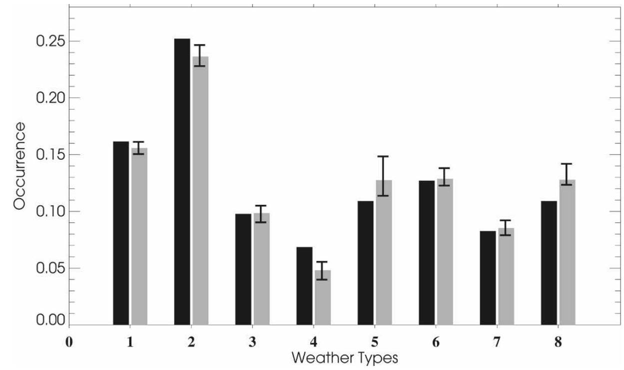

FIG. 10. Mean WT occurrence frequencies for the 1951–2000 period: observation (black) ensemble mean for the model (all forcings; gray). The error bars indicate the minimum and the maximum value in the ensemble.

given by the SGS simulation is a linear combination of individual signal responses to SST and GHG plus SUL, it is possible to estimate the individual β coefficients from the S and SGS simulations (Stott et al. 2001, see their appendix B). Results of the detection for the SST and GHG plus SUL signals are shown in Fig. 11. For the two signals, the detection is conclusive because the β coefficients are positive and the 1D and 2D confidence intervals exclude 0. The best estimates of the coefficients are greater than 1 in two cases, but because the confidence ellipse includes the (1, 1) point, the amplitude of the simulated signals is coherent with the observed amplitudes.

This result suggests that both observed SST and GHG plus SUL signals are consistent with the decadal evolution of WT occurrence frequency during the second half of the century. Given the results of the previous sections, it gives an indirect indication of the impact of SST and GHG plus SUL on precipitation over France. The biases in the links between the WTs and precipitation in the model may explain why the consistency test fails when the detection algorithm is applied to the decadal mean of precipitation and not when it is applied to the decadal mean of the WT occurrence frequency. Indeed, even if within the model the links between the WTs and precipitation are quite correctly reproduced (not shown), discrepancies still exist, for example, in southeastern France. Nevertheless, it is important to note that concerning the trends in the 1950–2000 period, the contribution of GHG plus SUL is very limited; much of the signal is due to SST (not shown). The simulated trends in WT occurrence frequency have much smaller amplitudes than that observed. The SST signal explains 35%, 30%, 20%, and 31% of the trends in WT2, WT3, WT4, and WT5 occurrence frequencies, respectively (for these WT, the observed trends are significant).

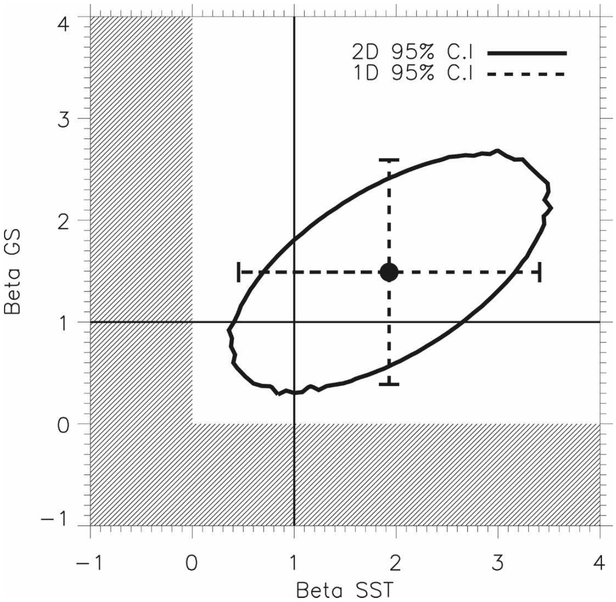

FIG. 11. Results of the optimal detection. The ellipse contains 95% of the estimated distribution of the β coefficients for the SST and GHG plus sulfate aerosols signals. The ellipse is centered on the best estimate of the two β coefficients (filled black circle). The one-dimensional confidence intervals at 95% of each β taken independently are shown by the horizontal and vertical dotted lines.

Note that given the experimental design, that is, the forced atmospheric approach, the SST signal may both incorporate the effect of natural SST variability and the effect of anthropogenic forcing on SST. Barnett et al. (2001) have shown that the observed ocean heat content changes are consistent with those expected from anthropogenic forcing. GHG plus SUL thus might have played an indirect role on the atmospheric circulation via its effect on SST. To go further, a coupled model approach should be followed. Given these results, it is not possible to confirm that anthropogenic forcing is responsible for the trends in WT occurrence frequency and precipitation.

8. Intratype variability and link with precipitation

In section 5, a linear regression model relating the November–March WT occurrence frequency to the November–March-accumulated precipitation amount was derived. This simple model captures an important part of the interannual variability of precipitation and the spatial pattern of precipitation trends during the second half of the twentieth century. Some discrepancies, however, exist with regard to the amplitude of the trends. In particular, the positive trends observed in northern France are greatly underestimated. The WT occurrence frequency does not explain all precipitation variability for two main reasons. First, regional precipitation is not totally explained by LSC. Quasi-identical synoptic situations may result in different precipitation intensities and patterns. Other processes are also important, notably those linked to the thermodynamic state of the atmosphere (stability, moisture availability, etc.). Second, considering only the WT occurrence frequency is a useful yet very simplified representation of the complex atmospheric circulation of the middle latitudes. Even if a WT groups days with similar circulation patterns, a dynamical intratype variability still exists. In this section, we try to better understand both the mechanisms that could explain the part of precipitation variability that is not linked to WT occurrence frequency and the discrepancies between the observed and reconstructed trends. However, given the lack of observations over a sufficiently long period for the many atmospheric variables required for a complete analysis, only qualitative results can be given.

a. Relationship between temperature and precipitation at the interannual level

Precipitation intensity is partly linked to the moisture availability in the atmosphere. Because the water-holding capacity of the atmosphere is greater for higher temperatures, as expressed by the Clausius–Clapeyron equation, there is generally a strong relationship between temperature and humidity, depending on the effective source of humidity. A potential relationship between precipitation and temperature can thus be postulated. Given the increasing trends in temperature over France (not shown), this could explain the discrepancy between observed and dynamically reconstructed trends.

First, the covariability between precipitation and temperature over France at the interannual level is examined. Because precipitation and temperature observations are not always available at the same location, for each precipitation station the nearest temperature station is examined. These distances are generally lower than 100 km (Fig. 12a). The correlation between November–March precipitation and the nearest temperature station is plotted in Fig. 12b. A north–south contrast is observed, with correlations generally greater than 0.35 and significant at the 0.01 level in the north and progressively decreasing southward, with near-zero or even negative correlation in the extreme south of France.

The correlation between temperature and precipitation should nevertheless be noted with caution. Indeed, the WTs associated with intense precipitation in northern France (see Fig. 3) correspond to westerly flow and

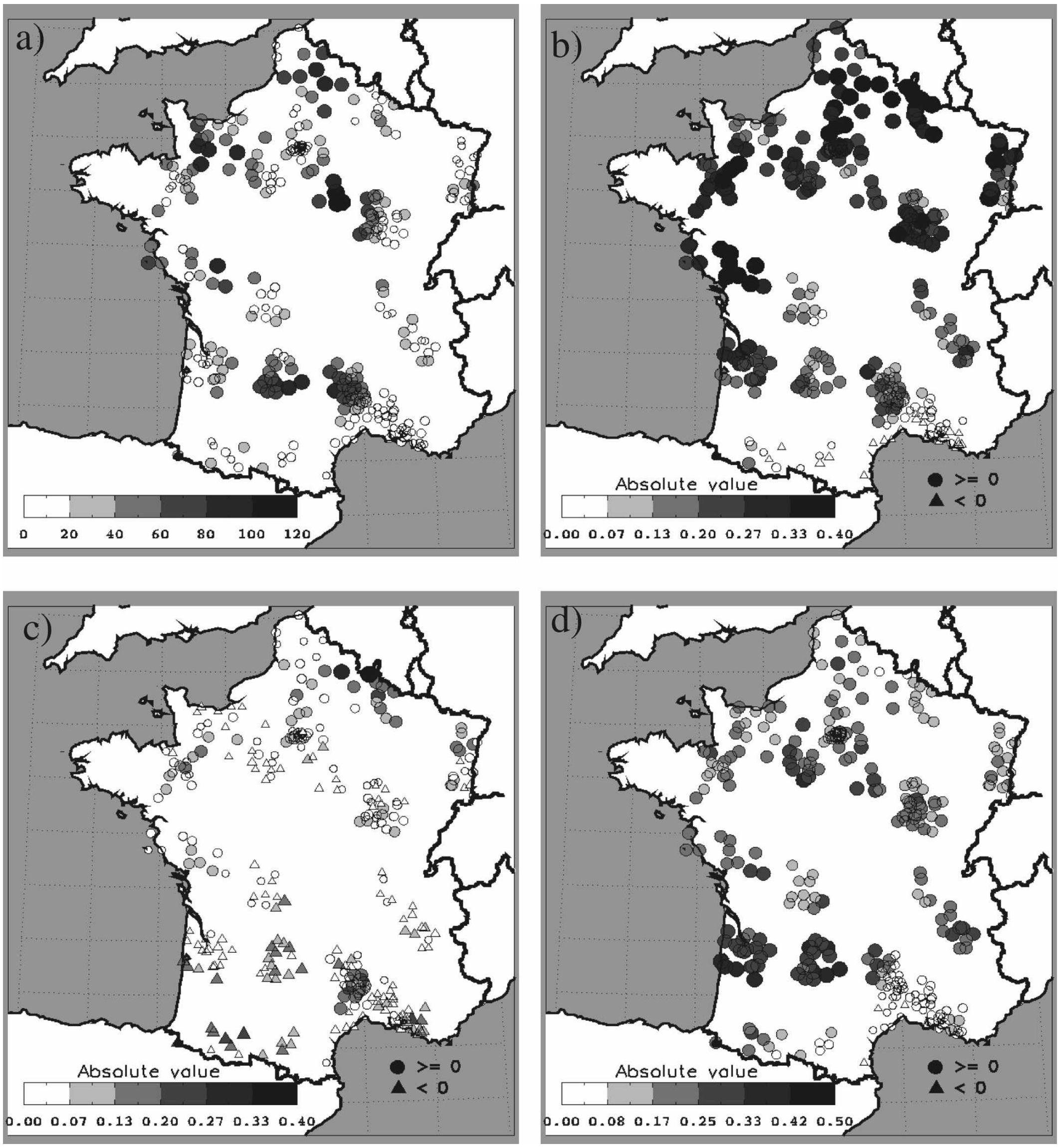

FIG. 12. (a) Distance (km) to the nearest temperature station from each precipitation station; (b) November–March correlation between precipitation and temperature; (c) November–March partial correlation between precipitation and temperature when removing the effect of WT occurrence frequency; and (d) difference between correlation and partial correlation.

thus to warm oceanic air advection in winter. The partial correlations between precipitation and temperature when removing the effect of WT occurrence frequencies are computed and compared to complete correlations (Figs. 12c,d). The partial correlations are much weaker than the total correlations, with many stations exhibiting a zero or even negative partial correlation. The partial correlations are generally not significant at the 0.01 level. This analysis shows that a major part of the covariability between precipitation and temperature in the twentieth century has a simple common cause, the LSC. Temperature thus does not provide important additional information regarding precipitation compared to WT occurrence frequency. At the interannual level, temperature is not a good secondary predictor of precipitation, when the WT occurrence frequency is already used. This nevertheless does not exclude the role of temperature in long-term precipitation changes in the global change context. For example, greater temperature could imply an increase of precipitation within some WTs. In section 8c we will test whether this hypothetical mechanism has played a role in precipitation changes during the second half of the twentieth century.

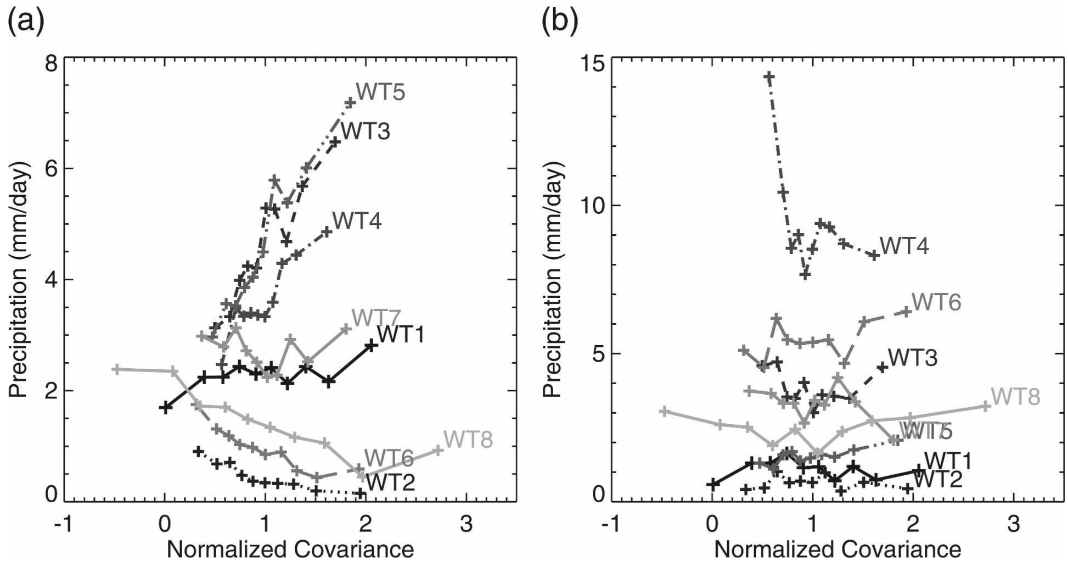

FIG. 13. Mean intratype precipitation given the covariance with the centroid of the WT: binned average of precipitation over 10 equally populated classes of covariances: (a) northeastern precipitation and (b) LRB region precipitation.

b. *Link between intratype dynamical variability and precipitation*

Here, intratype dynamical variability is investigated by only using MSLP based on the within-type distances to the centroid, because other dynamical variables are not available on the 1900–2000 period. We use the spatial covariance as a measure of similarity because it allows an easier physical interpretation. Indeed, the spatial covariance with the centroid well separates the days within a WT given the intensity of the MSLP anomaly for the given spatial pattern (not shown).

Figure 13 illustrates how the intratype variability of precipitation may be partly linked to intratype dynamical variability. For the sake of simplicity, only two precipitation series are considered here: averaged precipitation in the LRB region (a zone of strong decreasing trends) and averaged precipitation in the northeast (latitude greater than 47°N and longitude greater than 0°, which is the zone of strong increasing trends). First, within each WT, the spatial covariance between the MSLP of each day that belongs to the WT and the centroid are computed. Then, the covariances are classified into 10 equally populated bins. Finally, the mean covariance and the mean precipitation within each bin are computed. Results are encapsulated in Fig. 13. The link between the covariances with the WT centroid and the precipitation amount in the LRB region is very limited. Except for WT4, no clear relation can be deduced. On the contrary, with regard to northeastern precipitation, strong quasi-linear relationships are observed between the covariance and the precipitation intensity for a majority of WTs. For WT5, WT3, and WT4, which are responsible for the greater part of precipitation amount in this area, an increase of the covariance corresponds to a deepening of the negative associated MSLP anomalies (not shown), which is related to an increase of precipitation, as physically expected. Precipitation amounts are multiplied by a factor of 2 or 3 between the extreme bins. On the contrary, for WT2, WT6, and WT8, which are dry, the increase of the covariance is associated with stronger high pressures (in Europe for WT2, in northern Europe for WT6, and in eastern Europe for WT8), which corresponds to a decrease of northeastern precipitation (division by roughly a factor of 2 between the two extreme bins). For WT5 and WT3, the within-type covariance with the centroid exhibits a positive significant trend, which is consistent with an increase of precipitation in northeastern France (not shown). Within-pattern dynamical changes during the second-half of the twentieth century may thus have played a role regarding northeastern precipitation changes.

c. *Link with precipitation trends*

The possible influence of intratype dynamical and temperature changes on precipitation trends is now tested. As previously, multiple linear regressions are used to reconstruct November–March-accumulated precipitation amounts over the 1900–2000 period. The trends are then computed for the 1951–2000 period. In

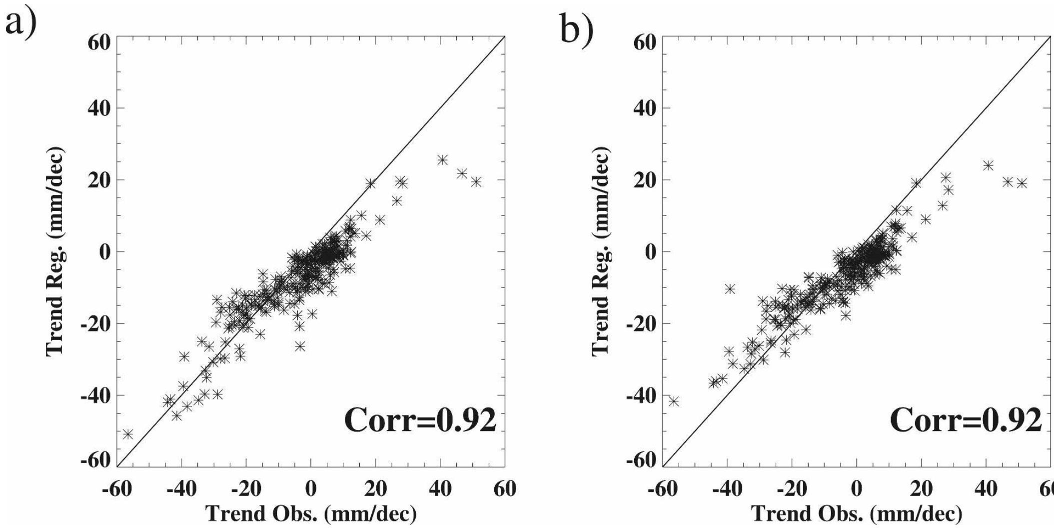

FIG. 14. Observed vs reconstructed by regression linear trends (mm decade^{-1}) in precipitation for the 1951–2000 period. The black line corresponds to the equation $y = x$. (a) WT occurrence frequency and covariances as predictors, and (b) WT occurrence frequency, covariances, and temperature as predictors.

the first case, the mean November–March covariances with the centroids are used as additional predictors for the November–March WT occurrence frequency. To limit the number of predictors, only the four most relevant WTs are kept in the analysis; WT3, WT4, WT5, and WT6 are chosen because they have the strongest links with precipitation. The second case is identical, except that temperature is used as additional predictor. The results are displayed in Fig. 14.

At the interannual level, the explained variance of November–March precipitation by the regression model is increased by 10% in the first case. As expected, the additional use of temperature in the second case does not result in a notable increase of the explained variance. A clear amelioration of the reconstructed trends is noted in the first case (Fig. 14a, cf. Fig. 7). In particular, the positive trends are less underestimated. The spatial pattern of reconstructed trends matches the observed one very well, with a spatial correlation of 0.92 (0.85 previously). With regard to the additional use of temperature as predictor (Fig. 14b), no clear amelioration is seen.

Intratype changes are of second order compared to intertype modifications. However, taking into account within-type dynamical changes, even partially by considering the similarity with the WT centroid, clearly improves the realism of trends in reconstructed precipitation. No effect of temperature is discernible.

9. Summary and conclusions

A long daily MSLP dataset has been used to derive eight WTs that are discriminant for winter (November–March) precipitation over France. The links between precipitation and the WTs have been studied for the entire twentieth century at different time scales. The "optimal detection algorithm" of Allen and Tett (1999) has been used to detect a possible anthropogenic influence on the decadal evolution of precipitation and WT occurrence frequency. Changes in precipitation that are not linked to changes in WT occurrence frequency have also been studied. The main conclusions are listed below, as follows: 1) the LSC (WT occurrence frequency) explains an important part of precipitation interannual variability in France; 2) the changes in WT occurrence frequencies well explain the spatial pattern of trends in precipitation during the second half of the twentieth century, with an increase (decrease) of precipitation in northern France (southern France), respectively (However, the changes in WT occurrence frequency are not sufficient to explain the magnitude of precipitation trends in the north.); 3) although both SST and anthropogenic GHG plus SUL emissions may have played a role in the decadal evolution of WT occurrence frequencies during the second half of the century, the role of GHG plus SUL in the trends is very limited; 4) changes in SST explain a part of the trends in WT occurrence frequency; 5) temperature change does not seem to have played a role in precipitation change during the 1951–2000 period; and 6) intratype circulation changes have played a role on precipitation changes, in particular in northeastern France, although intratype changes are of second order compared to intertype changes.

The detection study demonstrates that the variable-resolution version of the ARPEGE model has a realistic dynamical response to SST and anthropogenic forcing in the European sector. Given the strong relationship between regional climate and LSC, it provides confidence in both the regional climate change scenarios that are simulated by this model and their suitability for statistical downscaling. The relevance of the weather-typing approach to derive high-resolution information about precipitation changes over France has been demonstrated. Considering only intertype changes is, however, not sufficient to capture the entire climate change signal, in agreement with some previous results (e.g., Wilby et al. 2004). Considering intratype changes based on the distances to the WTs may be useful in this context.

Acknowledgments. This work was supported by the European Community via the sixth framework program ENSEMBLES project under Contract GOCE-CT-2003-505539 and by the French DISCENDO and RIVAGES research projects. Thanks are expressed to the EMULATE project participants for providing the North Atlantic mean sea level pressure data. Some statistical calculations of this study have been performed with Statpack, developed by P. Terray (IPSL/LOCEAN). The authors thank C. Cassou and J. Najac for stimulating discussion about this work and D. Stone and M. Allen for providing the optimal detection package.

APPENDIX

Optimal Detection Algorithm

A complete description of the algorithm is presented in Allen and Tett (1999) and Tett et al. (2002). Herein, only a concise description is given. Optimal detection is a form of multivariate regression. The vector of observations y is represented as a linear combination of a number of model-predicted vector signals x_i and intrinsic internal atmospheric variability u,

$$y = \sum_i \beta_i x_i + u. \tag{A1}$$

Here, β is estimated with the best linear unbiased estimator (BLUE). This algorithm is optimal as a signal-to-noise optimization is applied. Higher weighting is given to the region of phase space where the signal is dominant over noise because of natural variability. The optimization maximizes the chances of a successful outcome. First, it is checked whether the linear model provides a plausible representation of the observations by testing whether the residual u is consistent with the intrinsic internal atmospheric variability. A different estimation of the intrinsic internal atmospheric variability is then used to estimate the uncertainty in the β coefficients. In the two cases, the intrinsic internal atmospheric variability is estimated by the model because the length of the observations is not sufficient to provide a robust estimate. A second problem with the observations is that they may incorporate the anthropogenic signal. A signal is said to be detected when the associated β coefficient is found to be positive and inconsistent with zero. A β equal to 1 means that the amplitude of the signal is correctly estimated by the model, whereas a β greater (smaller) than 1 means that the signal is underestimated (overestimated) in the model.

In our case, intraensemble variability is used to estimate internal variability. The ensemble mean is removed from the six members for each ensemble of simulations. All of the obtained vectors are concatenated together and 10-yr overlapping segments are oversampled to increase the sample size. Two segments of equal length are then used to provide the two independent estimations of natural variability. Tett et al. (1999) note that when the different signals are too similar, the input signals are degenerated. This may lead to unrobust regression results, and thus compromise the detection. They propose three simple tests for signal degeneracy. Given these tests, only two signals can be studied simultaneously in our case. The study is therefore focused on SST and GHG plus SUL signals.

Under the hypothesis that the combined signal given by the SGS simulation is a linear combination of individual signal responses to SST and GHG plus SUL, it is possible to estimate the individual β coefficients (Stott et al. 2001). The best estimate of pure SST effect β_{SST} and GHG plus SUL effects β_{GS} are given by

$$\beta_{\mathrm{SST}} = \beta_S + \beta_{\mathrm{SGS}} \tag{A2}$$

and

$$\beta_{\mathrm{GS}} = \beta_{\mathrm{SGS}}, \tag{A3}$$

where the subscript S stands for the S simulations (forced by SST), and SGS stands for the SGS simulations (forced by SST and GHG plus SUL).

REFERENCES

Allen, M. R., and S. F. B. Tett, 1999: Checking for model consistency in optimal fingerprinting. *Climate Dyn.,* **15,** 419–434.

Ansell, T. J., and Coauthors, 2006: Daily mean sea level pressure reconstructions for the European–North Atlantic region for the period 1850–2003. *J. Climate,* **19,** 2717–2742.

Barnett, T. P., D. W. Pierce, and R. Schnur, 2001: Detection of anthropogenic climate change in the world's oceans. *Science,* **292,** 270–274.

——, and Coauthors, 2005: Detecting and attributing external influences on the climate system: A review of recent advances. *J. Climate,* **18,** 1291–1314.

Corte-Real, J., B. Qian, and H. Xu, 1998: Regional climate change in Portugal: Precipitation variability associated with large-scale atmospheric circulation. *Int. J. Climatol.,* **18,** 619–635.

Corti, S., F. Molteni, and T. N. Palmer, 1999: Signature of recent climate change in frequencies of natural atmospheric circulation regimes. *Nature,* **398,** 799–802.

Fowler, H. J., and C. G. Kilsby, 2002: Precipitation and the North Atlantic Oscillation: A study of climatic variability in Northern England. *Int. J. Climatol.,* **22,** 843–866.

Gibelin, A. L., and M. Déqué, 2003: Anthropogenic climate change over the Mediterranean region simulated by a global variable resolution model. *Climate Dyn.,* **20,** 327–339.

Gillett, N. P., F. W. Zwiers, A. J. Weaver, and P. A. Stott, 2003: Detection of human influence on sea-level pressure. *Nature,* **422,** 292–294.

——, R. J. Allan, and T. J. Ansell, 2005: Detection of external influence on sea level pressure with a multi-model ensemble. *Geophys. Res. Lett.,* **32,** L19714, doi:10.1029/2005GL023640.

Goodess, C. M., and P. D. Jones, 2002: Links between circulation and changes in the characteristics of Iberian rainfall. *Int. J. Climatol.,* **22,** 1593–1615.

Hurrell, J. W., 1995: Decadal trends in the North Atlantic Oscillation: Regional temperatures and precipitation. *Science,* **269,** 676–679.

Lambert, F. H., P. A. Stott, M. R. Allen, and M. A. Palmer, 2004: Detection and attribution of changes in 20th century land precipitation. *Geophys. Res. Lett.,* **31,** L10203, doi:10.1029/2004GL019545.

Mestre, O., 2000: Méthodes statistiques pour l'homogénéisation de longues séries climatiques. Ph.D. thesis, Université Paul Sabatier, 229 pp.

Michelangeli, P.-A., R. Vautard, and B. Legras, 1995: Weather regimes: Recurrence and quasi stationarity. *J. Atmos. Sci.,* **52,** 1237–1256.

Mitchell, T. D., T. R. Carter, P. D. Jones, M. Hulme, and M. New, 2004: A comprehensive set of high-resolution grids of monthly climate for Europe and the globe: The observed record (1901–2000) and 16 scenarios (2001–2100). Tyndall Centre Working Paper 55, 30 pp.

Moisselin, J.-M., M. Schneider, C. Canellas, and O. Mestre, 2002: Changements climatiques en France au 20ème siècle. Etude des longues séries de données homogénéisés françaises de précipitations et températures. *Météorologie,* **38,** 45–56.

Norrant, C., and A. Douguédroit, 2006: Monthly and daily precipitation trends in the Mediterranean (1950–2000). *Theor. Appl. Climatol.,* **83,** 89–106.

Paredes, D., R. M. Trigo, R. Garcia-Herrera, and I. F. Trigo, 2006: Understanding precipitation changes in Iberia in early spring: Weather typing and storm-tracking approaches. *J. Hydrometeor.,* **7,** 101–113.

Plaut, G., E. Schuepbach, and M. Doctor, 2001: Heavy precipitation events over a few Alpine sub-regions and the links with large-scale circulation, 1971–1995. *Climate Res.,* **17,** 285–302.

Sanchez-Gomez, E., and L. Terray, 2005: Large-scale atmospheric dynamics and local intense precipitation episodes. *Geophys. Res. Lett.,* **32,** L24711, doi:10.1029/2005GL023990.

Sexton, D., D. P. Rowell, C. K. Folland, and D. J. Karoly, 2001: Detection of anthropogenic climate change using an atmospheric GCM. *Climate Dyn.,* **17,** 669–685.

Smith, T. M., and R. W. Reynolds, 2004: Improved extended reconstruction of SST (1854–1997). *J. Climate,* **17,** 2466–2477.

Spagnoli, B., S. Planton, M. Déqué, O. Mestre, and J.-M. Moisselin, 2002: Detecting climate change at a regional scale: The case of France. *Geophys. Res. Lett.,* **29,** 1450, doi:10.1029/2001GL014619.

Stephenson, D. B., V. Pavan, and R. Bojariu, 2000: Is the North Atlantic Oscillation a random walk? *Int. J. Climatol.,* **20,** 1–18.

Stott, P. A., S. F. B. Tett, G. S. Jones, M. R. Allen, W. J. Ingram, and J. F. B. Mitchell, 2001: Attribution of twentieth century temperature change to natural and anthropogenic causes. *Climate Dyn.,* **17,** 1–21.

Straus, D. M., and F. Molteni, 2004: Circulation regimes and SST forcings: Results from large GCM ensembles. *J. Climate,* **17,** 1641–1656.

Terray, L., M.-E. Demory, M. Déqué, G. de Coetlogon, and E. Maisonnave, 2004: Simulation of late-twenty-first-century changes in wintertime atmospheric circulation over Europe due to anthropogenic causes. *J. Climate,* **17,** 4630–4635.

Tett, S. F. B., P. A. Stott, M. R. Allen, W. J. Ingram, and J. F. B. Mitchell, 1999: Causes of twentieth-century temperature change near the Earth's Surface. *Nature,* **399,** 569–572.

——, and Coauthors, 2002: Estimation of natural and anthropogenic contributions to twentieth century temperature change. *J. Geophys. Res.,* **107,** 4306, doi:10.1029/2000JD000028.

Trigo, R. M., and C. C. DaCamara, 2000: Circulation weather types and their influence on the precipitation regime in Portugal. *Int. J. Climatol.,* **20,** 1559–1581.

Von Storch, H., and F. W. Zwiers, 1999: *Statistical Analysis in Climate Research.* Cambridge University Press, 484 pp.

Wilby, R. L., S. P. Charles, E. Zorita, B. Timbal, P. Whetton, and L. O. Mearns, cited 2004: Guidelines for use of climate scenarios developed from statistical downscaling methods. Data Distribution Centre of the Intergovernmental Panel on Climate Change, 27 pp. [Available online at http://www.ipcc-data.org/guidelines/dgm_no2_v1_09_2004.pdf.]

Xoplaki, E., J. F. González-Rouco, J. Luterbacher, and H. Wanner, 2004: Wet season Mediterranean precipitation variability: Influence of large-scale dynamics and trend. *Climate Dyn.,* **23,** 63–78.

Zhang, X., X. L. Wang, and J. Corte-Real, 1997: On the relationship between daily circulation patterns and precipitation in Portugal. *J. Geophys. Res.,* **102,** 13 495–13 507.